

Comparison of denture models by means of micro computed tomography

Christoph Vögtlin^a, Georg Schulz^a, Hans Deyhle^a, Kurt Jäger^a, Thomas Liebrich^b,
Sascha Weikert^b, and Bert Müller^a

^aBiomaterials Science Center, University of Basel, 4031 Basel, Switzerland;

^bIWF / inspire AG, ETH Zürich, 8092 Zürich, Switzerland

ABSTRACT

The production of dental inlays and crowns requires precise information on patients' teeth morphology. The conventional method is the preparation of impressions using mold materials, e.g. a silicone impression material. The disadvantage of this technique is the human choke impulse and the flavor of the material. These discomforts can be avoided by methods where a three-dimensional scanner is used for recording the teeth morphology. The present study reveals the accuracy of three model types, namely conventional impression, rapid prototyping using an oral scanner C.O.S., 3M (Schweiz) AG and milling from a proprietary resin using the oral scanner iTero, Straumann Holding AG. For each method five models were fabricated from a steel reference (standard). Using a nanotom m (phoenix|x-ray, GE Sensing & Inspection Technologies GmbH), three-dimensional micro computed tomography data sets of the standard and the 15 models were recorded and landmark distances within the data sets were measured with sub-pixel accuracy. To verify these results a coordinate measuring machine (Leitz PMM 864, Hexagon Metrology GmbH) based on tactile detection was used for the measurement of the landmark distances, and a correction of the distances measured by the nanotom m was arranged. The nanotom data sets of the 15 models were also compared to the standard by means of a non-rigid registration algorithm. The calculated deformation field exhibited mean pixel displacement values of (0.19 ± 0.09) mm for the C.O.S. models, (0.12 ± 0.07) mm for the gypsum models and (0.19 ± 0.12) mm for the i-Tero models.

Keywords: dentistry, impression materials, intraoral scanner, micro computed tomography, tactile distance measurement, three-dimensional non-rigid registration

1. INTRODUCTION

The production of a fixed prosthetic restoration requires an accurate impression and master model which fulfills the requirements of the dental lab. Therefore, it is relevant to identify appropriate fabrication methods to produce reasonably accurate replicas of patients' jaws, particularly of the prepared teeth. The precision of a master impression and model is of major importance because the exact marginal, interdental and intermaxillary fit of the resulting laboratory restoration is only as precise as the master model. The master model takes a central role in the prosthetic treatment [1]. The conventional technique for the preparation of a gypsum model from elastomeric impressions has been in use since 1937, when Sears introduced agar as an impression material for crown preparation [2]. One of the first elastomeric materials specifically produced for dentists' needs was ImpregumTM, a polyether material introduced by 3M ESPE AG [3]. Until now, conventional plastic mold materials have been used to make an adequate impression of the patients' teeth. The first step in the prosthetic routine is to take an impression, e.g. using Alginate. The further impression for the master model requires an individual tray on the first plaster model. The impression materials (e.g. silicone, polysiloxane or polyether) combined with the individual tray lead to a higher quality with respect to the shape stability [4]. These materials provide highly accurate impressions of the prepared teeth and the dental environment. The accuracy of these conventional impression materials have been described in the literature for several times (e.g. [5, 6]). A disadvantage of this conventional method is the human choke impulse, which is aggravating for the patients and in some cases makes a fabrication of an impression impossible, and the flavor of the material. The

Further author information: (Send correspondence to G.S.)

E-mail: georg.schulz@unibas.ch, Telephone: +41 61 265 9127, Fax: +41 61 265 9699

Developments in X-Ray Tomography VIII, edited by Stuart R. Stock,
Proc. of SPIE Vol. 8506, 85061S · © 2012 SPIE · CCC code: 0277-786/12/\$18
doi: 10.1117/12.930068

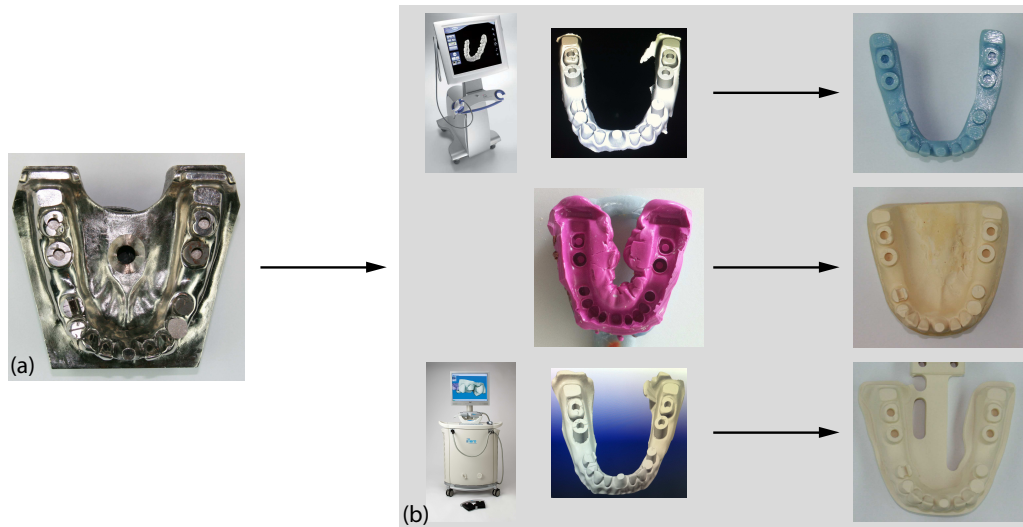


Figure 1. The photograph (a) shows the metallic standard used. By two digital and one conventional impression methods 15 master models were produced (b): five C.O.S. (top), five gypsum (middle) and five iTero (bottom).

physical properties of the mold materials like shrinkage and elastic deformations can affect the accuracy of the impression [7]. These imperfections lead to time-consuming fine-tuning by the dentist. Therefore the impressions have to be used within hours after their preparation to generate a gypsum model. Before this, the impression tray has to be transported to the dental lab, independent on the type of the impression material. Using this master model the technician produces the prosthetic restoration.

More than 20 years ago, digital prosthodontics entered the market with the introduction of CEREC [8] and has become more and more important in dentistry [9–11]. Nowadays, many procedures in daily use are based on a digital workflow, e.g. CEREC, Straumann® CARES®, Guided Surgery. A lot of dentists manage their administrative daily routine with digital aids. These digital means have the intention to automatize and simplify the prosthetic treatments. More and more manufacturers are offering devices for digital impressions. In this study two different intraoral scanners were used to take an impression of a steel arch: 3M™ Lava™ Chairside Oral Scanner, 3M (Schweiz) AG, Rüschlikon, Switzerland (see Fig. 1 (b) top) and iTero™, Institut Straumann AG, Basel, Switzerland (see Fig. 1 (b) bottom). Both scanners are mobile units with a personal computer on a mobile tray and a hand piece that is connected via a wire to the computer on the tray. The scanner piece must get guided by the dentist's hand over the occlusion and the prepared teeth. The opposite jaw has to be scanned and a scan in centric occlusion enables the bite registration. Consequently an impression of the opposite jaw and a bite registration with plastic mold materials are not required. The scanned images (iTero) and the video (C.O.S.) can be observed on the screen which is integrated on the mobile scanner tray. This possibility of controlling the impression on the screen during the impression recording allows the immediate correction of failures occurring during the prosthetic treatment. A repetition of the whole impression which is sometimes necessary with the conventional method is not required anymore. Together with features like the possibility of controlling the space between the preparation and the teeth in the opposite jaw, the scanner thus improves the dentist's level of control. A further advantage of digital impression systems is that the conventional lab prescription is unnecessary as the relevant information can directly be saved and there is no physical impression that has to be disinfected and physically transported to the dental lab.

More recently several studies concerning digital impression methods were published (e.g. [12]). Ender and Mehl demonstrated in a study from 2011 that digital optical impressions of full arch models can achieve the accuracy of conventional impressions in an in vitro test [13]. Most of these studies examine the digital virtual impression but not the master models produced by means of these impressions. In many of the digital workflows, the prosthetic restoration is produced digitally by milling out from e.g. a zirconia block. Here, the frames have to be veneered by technician's hand with ceramic for an excellent aesthetic result. For this veneering the

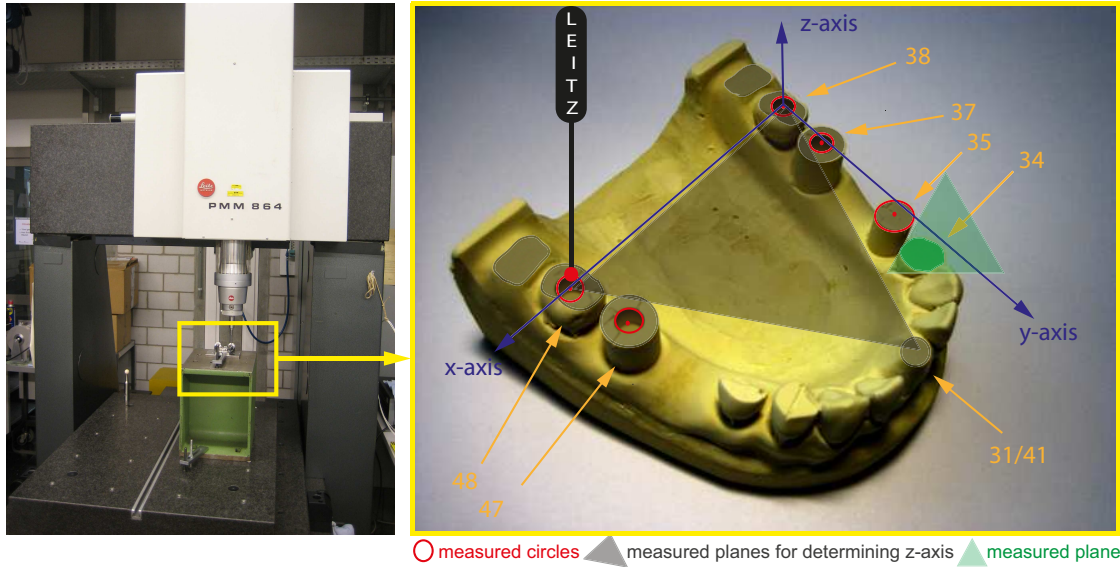


Figure 2. Photograph of the coordinate measuring machine Leitz PMM 864 (left) and the measuring plan for the determination of the distances in 3D (right). The teeth 38, 37, 35, 34, 31/41, 47 and 48 in this gypsum arch model (right) were dumped down to simple geometric bodies with circular forms (red circles) in order to simplify the measurement procedure.

master model plays an important role. An accurate master model is essential for the fabrication of prosthetic reconstructions with a clinically sufficient shape. Practical experience and literature demonstrate the hypothesis that the intraoral impressions have failures of superimposition in frontal regions which results in deformations of the molar regions [14]. The focus of the present study lies on the quantification of the imperfections of the master models produced after digital impressions.

For the present in vitro investigation a steel standard (Fig. 1 (a)) served as the reference for the different impression methods. Impressions were taken conventionally by A-silicone (Fig. 1 (b) left middle) and digitally by two intraoral scanners C.O.S. (Fig. 1 (b) left top) and iTero (Fig. 1 (b) left bottom). The deformations of the produced master models were quantified by measuring landmark distances using a coordinate measuring machine Leitz PMM 864 (see Fig. 2) and micro computed tomography (μ CT). Using a three-dimensional (3D) non-rigid registration of the μ CT data sets a 3D deformation field was calculated [15].

2. MATERIALS AND METHODS

A steel reference jaw standard (Fig. 1 (a)) served as a starting point for the present in vitro study. The shapes of the teeth 38, 37, 35, 34, 31/41, 47 and 48 of this model were simplified to geometric bodies like cylinders or a cone (Fig. 2). In each molar a cylinder with a diameter of 4 mm and a depth of 4 mm was eroded. Tooth 35 has a cylindrical shape. Furthermore, tooth 34 was shortened by about 1 mm (green plane in Fig. 2) with respect to the plane through the teeth 38, 37, 35, 31, 47, 46 (gray colored plane in Fig. 2).

2.1 Model preparation

Three impression methods, one conventional and two digital ones, were used to produce master models of the reference steel arch. Five A-silicone impressions (Heraeus Flexitime[®] monophasic, Heraeus Kulzer AG, Dübendorf, Switzerland) were taken with five individual trays. Using these impressions five gypsum models class IV (Fujirock[®], GC Europe, Leuven, Belgium) were manufactured in a dental lab. Finally, five models were produced by scanning the standard with the iTero[™] (Institut Straumann AG, Basel, Switzerland). The standard was scanned five times. After that the models were fabricated by Cadent Inc. (Or Yehuda, Israel) by milling out from a proprietary resin. A similar procedure was used for the impressions with the C.O.S. intraoral

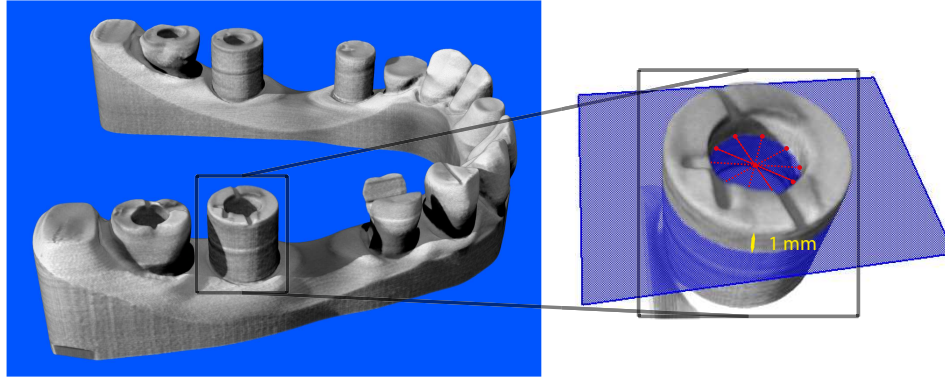


Figure 3. Selected 3D rendering of the μ CT data set of a C.O.S model (left). The virtually extracted tooth shows the top surface plane translated 1 mm in the direction of the first momentum of inertia of the cylinder and the center of the circle which was used for the determination of the landmark distances.

LAVATM scanner (3M (Schweiz) AG, Rüslikon, Switzerland). The master model was again scanned five times after powdering the standard with a fine grained titania powder which is necessary before scanning with the C.O.S. Lava scanner [16]. The model production was performed by 3M (Schweiz) AG, Rüslikon, Switzerland with rapid prototyping. Both model types (iTeroTM and C.O.S.) were produced without saw cuts in order to avoid any deformation.

2.2 Micro computed tomography

All the μ CT measurements were performed using a nanotom m (phoenix|x-ray, GE Sensing & Inspection Technologies GmbH, Wunstorf, Germany) equipped with a 180 kV / 15 W nanofocus X-ray source. During the scans the specimens were fixed on the precision rotation stage. 1440 equiangular radiographs were taken over 360°. For the metal standard an accelerating voltage of 180 kV and a beam current of 30 μ A were used. The gypsum models were scanned using an accelerating voltage of 150 kV and a beam current of 50 μ A, whereas for the scans of the iTero and the C.O.S. models an accelerating voltage of 80 kV and a beam current of 230 μ A were applied. In order to increase the mean photon energy, a 0.25 mm Cu filter was introduced. The exposure times were adjusted individually: 1.00 s for the metal standard, 0.75 s for the gypsum models and 1.50 s for the iTero and C.O.S. casts. For each projection three images were recorded and averaged in order to increase the signal-to-noise ratio. After the twofold binning to reduce the size of the data sets and to improve the density resolution [17], the camera readout (3072 \times 2400 pixels) resulted in a pixel length of 80 μ m. The projections were reconstructed using a cone beam filtered back-projection algorithm using phoenix datos|x 2.0.1 - RTM (GE Sensing & Inspection Technologies GmbH, Wunstorf, Germany).

2.3 Coordinate measuring Leitz PMM 864

The coordinate measuring machine (CMM) Leitz PMM 864 (Hexagon Metrology GmbH, Wetzlar, Germany (Fig. 2)) determined the coordinates of points on a surface by probing the surface with a probing element; in this work a probing sphere made of ruby with a diameter of 2 mm was used. This contact between the probing element and the model was detected and resulted in coordinates of single probing points. During probing, the probing force was set to 20 mN. The software used for controlling the coordinate measuring machine was Quindos (Hexagon Metrology GmbH, Wetzlar, Germany). The maximum permissible error for length measurement (MPE_E) of indication of the coordinate measuring machine used for size measurements with dimensions of the measured models was determined to be 1.6 μ m according to the ISO series 10360 [18]. The different eroded circles in the teeth were measured on a circle in 1 mm depth. On the basis of 16 probing points per circle the center points were determined, see Fig. 3. To estimate the measurement uncertainties for determining the position of the measured circles, a Monte-Carlo simulation was used. Therefore, the coordinates of each probing point were chosen at random from a uniform distribution with range of the MPE_E of 1.6 μ m with respect to their nominal coordinates. For each of the 1000 runs, the positions of the best fit circle through the simulated

Table 1. Calculated distances using Leitz PMM 864.

	38-37	48-47	38-48	37-47	38-35	48-35	z-dist.
	[mm]						
C.O.S. 1	10.309	10.124	48.472	44.390	28.210	50.132	0.937
C.O.S. 2	10.209	10.020	47.917	43.861	27.855	49.480	0.883
C.O.S. 3	10.343	10.155	48.635	44.454	28.303	50.210	0.896
C.O.S. 4	10.270	10.093	48.450	44.305	28.098	49.978	0.986
C.O.S. 5	10.286	10.104	48.715	44.550	28.120	50.170	0.869
Gypsum 1	10.306	10.132	48.777	44.541	28.218	50.221	0.851
Gypsum 2	10.308	10.142	48.794	44.562	28.230	50.243	0.837
Gypsum 3	10.311	10.143	48.793	44.558	28.235	50.246	0.850
Gypsum 4	10.312	10.140	48.787	44.552	28.236	50.237	0.844
Gypsum 5	10.311	10.142	48.803	44.567	28.232	50.249	0.851
iTero 1	10.271	10.125	48.794	44.629	28.145	50.180	0.771
iTero 2	10.307	10.120	48.696	44.484	28.156	50.152	0.866
iTero 3	10.230	10.119	48.710	44.563	28.257	50.022	0.807
iTero 4	10.279	10.103	48.721	44.521	28.219	50.116	0.794
iTero 5	10.252	10.131	48.576	44.407	28.138	50.178	0.838
Metal	10.301	10.132	48.768	44.535	28.214	50.214	0.843

measurement points were calculated. Therewith, the measurement uncertainties can be estimated by determining the standard deviations of the calculated positions. The expanded measurement uncertainty (coverage factor $k = 2$) for determining the diameter of a circle with 16 probing points on the CMM used was estimated to be $0.4 \mu\text{m}$, the expanded measurement uncertainty ($k = 2$) for determining the position was estimated to be $0.3 \mu\text{m}$. To affirm the high repeatability of the measurements (with an error smaller than $0.6 \mu\text{m}$) and the independence of the three-dimensional model position during the measuring procedure, the steel reference was measured three times without changing the mounting and one time with a 90° rotated orientation.

2.4 Data treatment

For the determination of the circle positions Matlab 7.8 (MathWorks, Natick, USA) was used. First the top of the individual tooth was detected. In order to obtain the same position as in the coordinate measurements (Fig. 3 right) this plane was shifted down by 1 mm. After that, the center of the eroded cylinder was determined by the calculation of the center of mass of this cylinder. The coordinates of the center of the circle then relate to the intersection of the blue colored plane (Fig. 3) and the line through this center of mass in the direction of the first moment of inertia of the eroded cylinder. For tooth 35 the same procedure was performed using the whole cylinder.

In addition to this, the analysis of the local deformations was performed by means of a 3D non-rigid registration of the data sets as was done with 2D data sets by Germann *et al.* [19] and 3D data sets by Schulz *et al.* [15,20]. Before the registration, a threshold value was set for the segmentation of material and air between the well separated material peaks [21].

For the visualization of the 3D data sets and the 3D local deformation field the software VG Studio Max 2.0 (Volume Graphics GmbH, Heidelberg, Germany) was used.

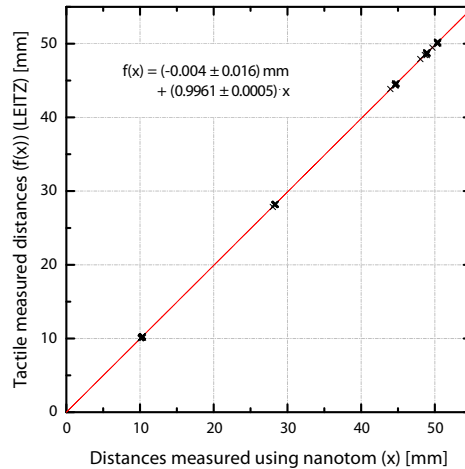


Figure 4. For the evaluation of the distances measured by nanotom m, all these distances were plotted against the distances measured with Leitz PMM 864. The distances calculated by the nanotom m were corrected using the line of best fit.

3. RESULTS

3.1 Tactile measurements

The tactile coordinate measurements served for the comparison of distances between the centers of the predefined teeth. Table 1 compares the data of the 15 master models, consisting of five C.O.S., five gypsum and five iTero, with the reference steel standard. The repeated measurements allow for the determination of standard deviations, which characterize the reliability of the procedures, whereas the differences between the standard and the means characterize the accuracy of the selected method. The conventional approach (gypsum) provided better values concerning reliability and accuracy, but the scanners also yielded highly precise data.

3.2 Micro computed tomography

The results obtained by μ CT provided 3D data sets of the 16 specimens. The left image in Fig. 3 shows a 3D rendering of a selected C.O.S. data set. After calculating the same distances as for the tactile measurement the values were correlated and calibrated using the parameters a and b of the line of best fit shown in Fig. 4. The corrected distances of the μ CT data are listed in Tab. 2 to get an impression on the precision and reliability of the three procedures.

3.3 Non-rigid 3D registration

In order to quantify the local imperfections of the models with respect to the steel standard, the μ CT data sets were non-rigidly registered in 3D space [15]. The reference was always the data set of the steel standard. The results are shown for the three fabrication routes in Fig. 5 by color-coded virtual arch models. The colors relate to differences between the models and the measured standard. Cold colors represent small pixel displacements whereas red corresponds to maximal differences. The pixel displacements are quantified in Fig. 6. Here, the diagonally shaded bars correspond to mean values of the pixel displacement (the error bar shows the standard deviation) of each object and the entire fabrication type (named total in the figure), while the checked bars show maximal values of each model plus the maximal values of the 3 entire fabrication types. The displacement values of the model iTero 5 are not shown as the registration failed. Fig. 5 and 6 demonstrate that the data of the scanners are comparable and only slightly worse than the conventional approach (gypsum). The scattering between different models of one fabrication route, however, are larger for the scanners.

Table 2. Calculated distances using nanotom m after correction by the line of best fit of Fig. 4.

	38-37	48-47	38-48	37-47	38-35	48-35	z-dist.
	[mm]						
C.O.S. 1	10.309	10.121	48.450	44.373	28.219	50.088	0.897
C.O.S. 2	10.221	10.033	47.844	43.791	27.901	49.474	1.002
C.O.S. 3	10.348	10.154	48.765	44.547	28.282	50.247	0.915
C.O.S. 4	10.274	10.091	48.708	44.483	28.115	50.110	0.999
C.O.S. 5	10.302	10.121	48.660	44.497	28.186	50.153	0.884
Gypsum 1	10.287	10.107	48.671	44.452	28.145	50.098	0.924
Gypsum 2	10.287	10.121	48.687	44.465	28.231	50.144	0.859
Gypsum 3	10.289	10.119	48.684	44.465	28.227	50.170	0.912
Gypsum 4	10.290	10.130	48.681	44.455	28.244	50.165	0.883
Gypsum 5	10.289	10.120	48.702	44.475	28.260	50.218	0.870
iTero 1	10.228	10.107	48.819	44.650	28.115	50.180	0.756
iTero 2	10.296	10.099	48.765	44.544	28.228	50.145	0.783
iTero 3	10.291	10.106	48.745	44.590	28.262	50.252	0.807
iTero 4	10.267	10.096	48.817	44.597	28.288	50.183	0.776
iTero 5	10.179	10.120	48.650	44.460	28.241	50.269	0.794
Metal	10.304	10.110	48.685	44.486	28.175	50.137	0.889

4. DISCUSSION

Anatomical structures such as ascending ramus or a limited mouth opening can complicate a correct impression. Also, sub-gingival preparations or a higher salivation can hinder the dentist when taking an accurate impression. To exclude this kind of external influence the steel model was a helpful instrument. In the recent literature there is general agreement that crowns produced by digital impression have a better fit than crowns based on conventional impressions [22]. This might be explained by the digital intraoral scan where the crown framework is designed directly from the intraoral data set without manufacturing an intermediate master model. In a recent study the accuracy of intraoral scans was confirmed [13]. The reduced marginal gap of crowns' frames is a big advantage in the digital workflow [22]. For most prosthetic restorations the framework has to be veneered manually by a technician. Therefore a master model is used for controlling the space between the neighboring teeth and the neighbor arch to produce crowns and bridges with a sufficient occlusal and approximate contact. The physiological mobility of a tooth with a healthy periodontium is between 30 and 100 μm [23]. Difference from a master model or a prosthetic restoration in this range can be considered as clinically sufficient. The largest deviation in distance between different neighboring teeth in a quadrant were below 100 μm . These distances are equivalent to the dimensions of two single crowns. This means that the master models are at least completely sufficient for the manufacturing of two dental restorations.

The possible error of the distances listed in Table 1 was determined to be 1.6 μm (cp. Sec. 2.3). Compared to that, the μCT data sets, with pixel sizes of 80 μm seem to have a restricted precision. However, the procedure for the calculation of the distances determined within the tomography data, where first the centers of the eroded cylinders were calculated by means of mean values of pixel positions located at the surface of the cylinder, reaches sub-pixel accuracy. Under the assumption that the μCT system describes the distances exactly, this method leads to error values of only around 1 μm because of the high amount of voxels (≈ 8000 voxels) used for the center positions determinations. As the precision of the nanotom might slightly deviate from the real situation, a calibration of the determined distances using standardized tactile instrumentation was performed (see. Fig. 4). Using the error values of the line of best fit, which was used for the correction of the nanotom distances, error

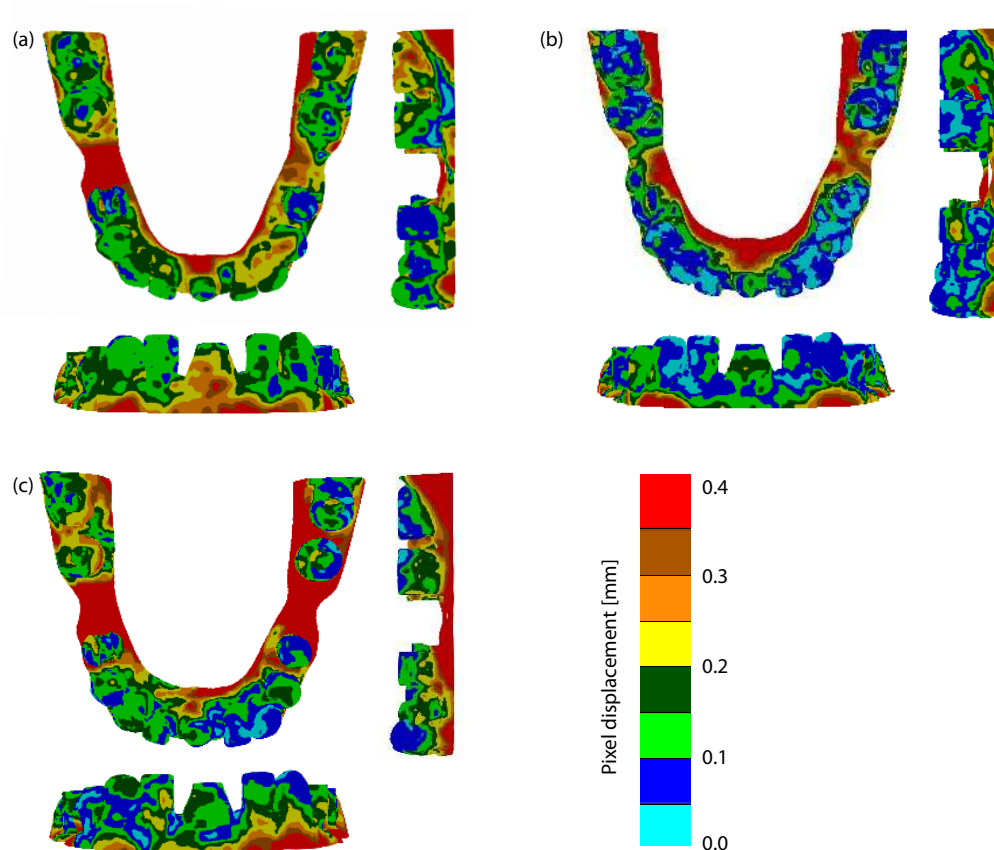


Figure 5. Pixel displacement field of the μ CT data sets in comparison to steel standard: (a) C.O.S., (b) gypsum, (c) iTero. The most accurate replicas with minimal mean pixel displacements are in the gypsum experimental group.

values for these distances can be calculated. These are higher than the $1 \mu\text{m}$, assumed for the optimal case, lying between $20 \mu\text{m}$ for short and $40 \mu\text{m}$ for longer distances. Nevertheless, the values listed in Table 2 are displayed with μm -precision, in order to show these values to interested readers although these last numbers are not really significant.

The gypsum models were larger than the steel standard. This magnification of the metric gypsum data can be explained by the expansion of the impression material Flexitime monophase and the gypsum Fujirock. Piowarczyk demonstrated in a study about the dimensional accuracy of monophase impression, that Flexitime monophase has a maximal contraction of 0.04% [5]. Furthermore, the expectable expansion of the gypsum Fujirock is about 0.08% [24]. A study by Caputi concerning the accuracy of monophase impressions from a steel standard similar to the reference used in this study demonstrated that all dimensions on the gypsum (Fujirock) models were greater than the corresponding dimensions on the steel standard [6]. The accuracy of an impression can also be analyzed by fitting of the resulting restoration but these results are influenced by diverse processes during the restoration production [22]. Several studies described the accuracy of conventional impression by means of linear distance measurements [6, 25]. Both tables (Tab. 1 and Tab. 2) show the expected high accuracy of the gypsum models. The largest deviations in the y-direction in the range of a 4 unit bridge (ca. 40 mm) are below $100 \mu\text{m}$ for C.O.S and iTero. That means the manufacturing of a 4 unit-restoration is clinically feasible. The models from digital scans, especially the model Nr. 2 from C.O.S., were compressed in transversal direction. Larger discrepancies were found for distance deviations in the z-direction. These deviations do not mean that prosthetic restorations manufactured by means of digital intraoral scans have a worse occlusal

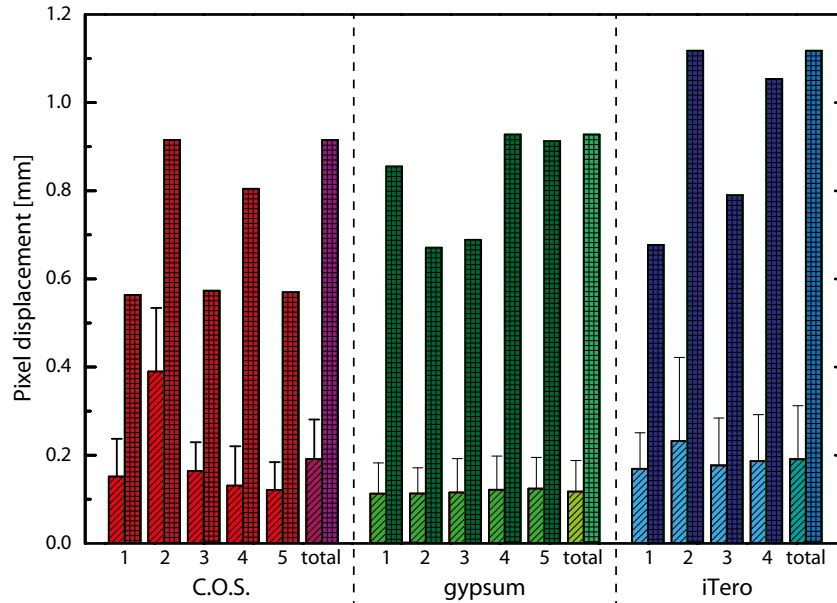


Figure 6. Pixel displacements of all data sets except data set of model iTero 5. The diagonally shaded bars represent the mean values of the pixel displacement values of the individual models as well as of the whole preparation type where the error bars show the standard deviation of the data sets. The maximal displacements are illustrated by the checked bars.

contact in comparison to gypsum models. The bite registration is taken during the scanning procedure in centric occlusion. No bite registration masses are between the lower and the upper jaw that may hamper the registration in perfect occlusion. However, the occlusal behaviour of a digitally manufactured crown is described by Syrek and Scotti as clinically sufficient [22,25]. To evaluate local deformations in the different master models a method other than the linear measurements is required. This effect is shown excellently by Fig. 5. The color-coded illustrations demonstrate the compression effect. The reasons for these deformations could be a superimposition in frontal regions during a full arch scan or a distortion of the master models during the production procedure. These transversal distances would be relevant for the manufacturing of full arch bridges but in the consideration of the fact, that e.g. the LAVA™ zirconia block has a size of 60 mm, the production of such a large reconstruction is infeasible today and it is irrelevant for the clinical acceptability.

In the present study the gypsum data sets show a high reliability. In comparison to the models produced by digital workflows, the gypsum models have smaller standard deviations of the local displacements, illustrated in Fig. 6. The automatic production of the master models from C.O.S and iTero by digital intraoral impression seems to have greater internal variances than the conventional method. Therefore, one may conclude that extensive learning curves on the part of the dentists are required to reach better reliability. Alternatively the suppliers of the scanners may improve their instrumentation and software to reach a better reliability. By contemplating the mean values of the calculated deformation fields exhibited mean pixel displacement values of (0.19 ± 0.09) mm for the C.O.S. models, (0.12 ± 0.07) mm for the gypsum models and (0.19 ± 0.12) mm for iTero models we can conclude that the two intraoral impression methods are similar and both almost reach the precision of the conventional gypsum models.

5. CONCLUSIONS

The combination of μ CT and appropriate software for 3D data evaluation one to construct a detailed isometric view of dental master models. This feedback is helpful for the optimization of the fabrication of master models based on digital intraoral scans. The present investigation also elucidates that μ CT and non-rigid registration algorithms are useful instruments for further studies concerning measurements of models relating to physiological or orthodontic tooth movements. The present study also elucidates that master models, produced using

digital data from intraoral scans, are clinically sufficient in spite of the less accurate reproduction of surfaces in comparison to conventional impressions and gypsum models. However, these in vitro data still have to be confirmed by in vivo studies on patients, see Brogle-Kim *et al.* in this volume [26].

ACKNOWLEDGMENTS

The author team gratefully acknowledges Emil Mangold AG, Oberdorf, Switzerland for the helpful construction of the steel reference and Straumann AG, Basel, Switzerland, 3M (Schweiz) AG, Rüschiikon, Switzerland and Zahntechnik Ess, Olten, Switzerland for the production of the master models. The authors especially acknowledge the financial support of the Swiss National Science Foundation in the frame of the R'Equip initiative (316030_133802).

REFERENCES

- [1] Wirz, J., Jäger, K., and Schmidli, F., [*Abformung in der zahnärztlichen Praxis*], Elsevier, München (1993).
- [2] Sears, A. W., "Hydrocolloid impression technique for inlays and fixed bridges," *Dent. Dig.* **43**, 230–234 (1937).
- [3] Brücking, W., "Die perfekte Abformung," *Quintessenz* **57**, 59–75 (2006).
- [4] Donovan, T. E. and Chee, W. W., "A review of contemporary impression materials and techniques," *Dent. Clin. North Am.* **48**, 445–470 (2004).
- [5] Piwowarczyk, A., Ottl, P., Büchler, A., Lauer, H. C., and Hoffmann, A., "In vitro study on the dimensional accuracy of selected materials for monophasic elastic impression making," *Int. J. Prosthodont.* **15**, 168–174 (2002).
- [6] Caputi, S. and Varvara, G., "Dimensional accuracy of resultant casts made by a monophasic, one-step and two-step, and a novel two-step putty/light-body impression technique: an in vitro study," *J. Prosthet. Dent.* **99**, 274–281 (2008).
- [7] Papadogiannis, D., Lakes, R., Palaghias, D., and Papadogiannis, Y., "Effect of storage time on the viscoelastic properties of elastomeric impression materials," *J. Prosthodont. Res.* **56**, 11–18 (2011).
- [8] Mörmann, W., "The evolution of the CEREC system," *J Am Dent Assoc.* **137 Suppl**, 7S–13S (2006).
- [9] Garg, A. K., "Cadent iTero's digital system for dental impressions: the end of trays and putty?," *Dent. Implantol. Update* **19**, 9–11 (2008).
- [10] Kachalia, P. and Geissberger, M. J., "Dentistry a la carte: in-office CAD/CAM technology," *J. Calif. Dent. Assoc.* **38**, 323–330 (2010).
- [11] Jäger, K. and Vögtlin, C., "Digitaler Workflow mit dem Lava Chairside Oral Scanner C. O. S und der Lava-Technik," *Schweiz. Monatsschr. Zahnmed.* **122**, 307–315 (2012).
- [12] Luthardt, R. G., Loos, R., and Quaas, S., "Accuracy of intraoral data acquisition in comparison to the conventional impression," *Int. J. Comput. Dent.* **8**, 283–294 (2005).
- [13] Ender, A. and Mehl, A., "Full arch scans: conventional versus digital impressions - an in vitro study," *Int. J. Comput. Dent.* **14**, 11–21 (2011).
- [14] Vauthier, T., Jung, R., Paul, S., Paqué, F., Mehl, A., Katsaros, C., Schulze, D., Marquardt, P., Sailer, I., and Edelhoff, D., "Vom Bohrer zur Maus," *Schweiz. Monatsschr. Zahnmed.* **121**, 1206–1210 (2011).
- [15] Müller, B., Deyhle, H., Lang, S., Schulz, G., Bormann, T., Fierz, F., and Hieber, S., "Three-dimensional registration of tomography data for quantification in biomaterials science," *Int. J. Mater. Res.* **103**, 242–249 (2012).
- [16] Rohály, J., "The development of the Lava chairside oral scanner C.O.S. technology—masterstroke of a legion of talented and committed people. Interview by Laslo Faith," *Int. J. Comput. Dent.* **12**, 165–169 (2009).
- [17] Thurner, P., Beckmann, F., and Müller, B., "An optimization procedure for spatial and density resolution in hard X-ray micro-computed tomography," *Nucl. Instrum. Methods Phys. Res., Sect. B* **225**, 599–603 (2004).
- [18] ISO 10360-1:2000, *Geometrical Product Specifications (GPS) - Acceptance and reverification tests for coordinate measuring machines (CMM) - Part 1: Vocabulary* (Geneva, Switzerland, 2000).

- [19] Germann, M., Morel, A., Beckmann, F., Andronache, A., Jeanmonod, D., and Müller, B., “Strain fields in histological slices of brain tissue determined by synchrotron radiation-based micro computed tomography,” *J. Neurosci. Methods* **170**, 149–155 (2008).
- [20] Schulz, G., Crooijmans, H. J., Germann, M., Scheffler, K., Müller-Gerbl, M., and Müller, B., “Three-dimensional strain fields in human brain resulting from formalin fixation,” *J. Neurosci. Methods* **202**, 17–27 (2011).
- [21] Müller, B., Beckmann, B., Huser, M., Maspero, F., Székely, G., Ruffieux, K., Thurner, P., and Wintermantel, E., “Non-destructive three-dimensional evaluation of a polymer sponge by micro-tomography using synchrotron radiation ,” *Biomol. Eng.* **19**, 73–78 (2002).
- [22] Syrek, A., Reich, G., Ranftl, D., Klein, C., Cerny, B., and Brodesser, J., “Clinical evaluation of all ceramic crowns fabricated from intraoral impressions based on the principle of active wavefront sampling,” *J. Dent.* **38**, 553–559 (2010).
- [23] Ott, R., Vollmer, H. P., and Krug, W., [*Klinik- und Praxisführer Zahnmedizin*], Thieme, Stuttgart (2002).
- [24] GC EUROPE, “Three first class Type 4 Dental Die Stones: all-purpose, free-flowing or CAD/CAM-optimised,” tech. rep., www.gceurope.com/news/press/200903/en_fujirock.doc (2009).
- [25] Scotti, R., Cardelli, P., Baldissara, P., and Monaco, C., “Clinical fitting of CAD/CAM zirconia single crowns generated from digital intraoral impressions based on active wavefront sampling,” *J. Dent.* **in press** (2011).
- [26] Brogle-Kim, Y.-C., Deyhle, H., Müller, B., Schulz, G., Bormann, T., Hieber, S., Beckmann, F., and Jäger, K., “Evaluation of oral scanning in comparison to impression using three-dimensional registration,” *Proc. SPIE* **8506** (2012).